Submitted to *The Astrophysical Journal*

Theoretical Black Hole Mass Distributions

Chris L. Fryer
Lick Observatory, University of California Observatories,
Santa Cruz, CA 95064
cfryer@ucolick.org

Vassiliki Kalogera
Harvard-Smithsonian Center for Astrophysics, 60 Garden St., Cambridge, MA 02138
vkalogera@cfa.harvard.edu

ABSTRACT

We derive the theoretical distribution function of black hole masses by studying the formation processes of black holes. We use the results of recent 2D simulations of core-collapse to obtain the relation between remnant and progenitor masses and fold it with an initial mass function for the progenitors. We examine how the calculated black-hole mass distributions are modified by (i) strong wind mass loss at different evolutionary stages of the progenitors, and (ii) the presence of close binary companions to the black-hole progenitors. Thus, we are able to derive the binary black hole mass distribution. The compact remnant distribution is dominated by neutron stars in the mass range 1.2–1.6 $M_\odot$ and falls off exponentially at higher remnant masses. Our results are most sensitive to mass loss from winds which is even more important in close binaries. Wind mass-loss causes the black hole distribution to become flatter and limits the maximum possible black-hole mass ($\lesssim 10-15\,M_\odot$). We also study the effects of the uncertainties in the explosion and unbinding energies for different progenitors. The distributions are continuous and extend over a broad range. We find no evidence for a gap at low values ($3-5\,M_\odot$) or for a peak at higher values ($\sim 7\,M_\odot$) of black hole masses, but we argue that our black hole mass distribution for binaries is consistent with the current sample of measured black-hole masses in X-ray transients. We discuss possible biases against the detection or formation of X-ray transients with low-mass black holes. We also comment on the possibility of black-hole kicks and their effect on binaries.

Subject headings: black hole physics — stars: binaries — stars: evolution — stars: supernovae — stars: neutron — stars: mass loss

1. Introduction

Soft X-ray transients provide a window into the nature of compact objects, and in particular, stellar mass black holes. During the quiescent state of emission (low X-ray luminosity), optical/infrared observations of the compact object's companion allow the measurement of the mass function and other

binary parameters. In the case of small companion masses (late spectral type) the value of the mass function, $f(M_{\rm X})$, sets a strong lower limit to the mass of the compact object:

$$M_{\rm X} \;=\; f(M_{\rm X})\,\frac{(1+q)^2}{\sin^3 i} \;>\; f(M_{\rm X}), \tag{1}$$

where $q \equiv M_c/M_{\rm X}$ is the mass ratio, and i is the inclination of the binary orbit. For several systems, this lower limit exceeds $3\,{\rm M}_\odot$, the optimum (independent of the equation of state of matter at densities exceeding nuclear densities) upper limit to the gravitational mass of a neutron star (NS) (Rhoades & Ruffini 1974; Kalogera & Baym 1996), strongly suggesting that these compact objects are black holes (for a recent review see Charles 1998). Indeed, at present, there is little doubt that stellar mass black holes (BH) exist, and that they play an important role in high-energy astrophysics (e.g., X-ray binaries, gamma-ray bursts).

Currently there are 9 X-ray transients thought to contain a BH accreting matter from a low mass companion. They are listed in Table 1 along with the range of BH mass estimates reported in the literature. Most of the data have been taken from Bailyn et al. (1998) who presented a detailed statistical study of the BH mass measurements available at the time and the associated errors (dominated by uncertainties in the inclination angle). Recently, revised measurements of the mass function for GRO J1655-40 (Phillips, Shahbaz, & Podsiadlowski 1999) and GRO J0422+32 (Harlaftis et al. 1999) have led to a decrease in the lower mass limits. In Table 1 we also include two new systems 4U 1543-47 (Orosz et al. 1999) and GRS 1009-45 (Filippenko et al. 1999), although their mass estimates are still rather uncertain.

Bailyn et al. (1998) studied the statistical properties of the early sample of measured BH masses (excluding 4U 1543-47 and GRS 1009-45, and the revised masses for GS1124-68 and GRO J0422+32) and concluded that almost all of the estimates are consistent with a narrow range of BH masses around $7\,{\rm M}_\odot$ and that a gap between 3 and $5\,{\rm M}_\odot$ is present in the distribution. In this paper we calculate the expected BH mass distribution and its dependence on a number of physical elements (stellar winds and binary evolution) based on the current theoretical understanding of BH formation.

We consider BH formation during the collapse of massive stars. This process can proceed in two different ways: either the massive star collapses directly into a BH without a supernova explosion, or an explosion occurs, but its energy is too low to completely unbind the stellar envelope, and a significant part of the star falls back onto the proto-neutron star forming a BH (Colgate 1971; Woosley 1988; Fryer 1999a). An alternative path involving the collapse of a NS into a BH through hypercritical accretion (e.g., in a common envelope or in binary mergers) has often been discussed in recent years (see Fryer, Woosley, & Hartmann 1999 for a review). However, even under the assumption that BH formation occurs every time a NS goes through a common-envelope phase or a merger, the event rates for NS accretion-induced collapse are lower than those for massive star collapse events by factors of 10–100 (Fryer, Woosley, & Hartmann 1999). Therefore, we assume that BH formation is dominated by stellar collapse.

In this paper we use the results of up-to-date 2D hydrodynamic simulations of core collapse (Fryer 1999a) for explosion energies and remnant masses to obtain theoretically expected BH mass distributions. In § 2, we outline the steps involved in constructing such distributions and discuss their associated uncertainties. We present our results in § 3 and conclude that the BH mass distribution and particularly its slope and upper cut-off is most sensitive to the effects of stellar winds in binaries. No evidence for a gap is found at low BH masses. In the last section we compare our results to observations and discuss some possible biases and uncertainties in the observed sample.

2. Black Hole Mass Distributions

2.1. Outline of the Calculation

The calculation of theoretically expected BH mass distributions involves a sequence of steps. We derive the remnant mass as a function of progenitor mass[1] based on an energy-budget argument regarding the *necessary* and *available* energies to unbind the stellar envelope. We scale the available energy to the explosion energy calculated from core-collapse simulations. We then convolve the resulting remnant-progenitor mass relation with the initial mass function of the progenitors to obtain the BH mass distribution. Each of these steps, and hence the results, can be affected quantitatively by the evolution of the progenitor prior to collapse. Before we present our results and the associated uncertainties, we detail the steps of our calculation.

Explosion Energy. To estimate the energy available to unbind the stellar envelope and its dependence on progenitor properties (mass and density structure), we are guided by recent 2D core-collapse simulations (Fryer 1999a), which provide us with the explosion energy as a function of the progenitor mass. This explosion energy is determined by the change in total energy before collapse and at the end of the ∼1s simulation of the material that is initially part of the exploding shock (for most simulations, this is the entire star beyond the $1.2\,M_\odot$ proto-neutron star). Mass loss (from winds or binary mass transfer) will not change the explosion energies unless the mass-loss affects the inner $\sim 3\,M_\odot$ of the stellar core. Hence, the explosion energies as a function of progenitor mass from Fryer (1999a) are valid for both helium and hydrogen stars. For stars in which mass loss has affected the core, C/O cores at collapse have been calculated (Langer & Henkel 1995) and we use these masses to estimate the explosion energy. We find that mass loss affects the cores of stars only for a small fraction of the BH progenitors (more massive than $\sim 40\,M_\odot$). For example, a $40\,M_\odot$ star with winds from Langer & Henkel (1995) will have an explosion energy closer to that of a $30\,M_\odot$ progenitor star without winds. Such cases are discussed in more detail in § 2.2.3.

Knowing the explosion energy from core-collapse models is not sufficient to estimate the final compact remnant mass. We also need to know what fraction of the explosion energy goes into unbinding the star, and what fraction is transformed into kinetic energy of the ejecta. In Figure 1 we plot (dotted lines) two different examples of the energy available to unbind the star as a function of the progenitor mass. For the top curve, we assume that 100% of the collapse energy goes into unbinding the star and is a fit to the results (black dots) of Fryer (1999a). The lower curve is a scaled-down version of the top curve assuming that 10% of the explosion energy is used to unbind the star, the rest being transformed into kinetic energy of the ejecta. The simulations show that above a critical progenitor mass, no supernova occurs, and the entire star collapses to form a black hole. A progenitor of $\sim 40\,M_\odot$ appears to be the critical mass for BH formation (see Fryer 1999a for more details).

Stellar Binding Energy. The next step is to compare the energy available to eject material to the actual binding energy of the star, obtained from integrating the stellar mass profile. For these profiles we use the models of massive stars calculated by Woosley & Weaver (1995). In Figure 1 we plot (solid line) the energy required to unbind all but the inner $3\,M_\odot$ for each progenitor. We assume that the maximum NS mass is $3\,M_\odot$ and we thus calculate an *upper limit* to the critical initial progenitor mass dividing NS from BH formation through fallback. From Figure 1 it is evident that the critical masses are $\sim 18\,M_\odot$ and $\sim 23\,M_\odot$

[1]Since BH progenitors can lose mass as they evolve because of winds and binary mass transfer, the term "progenitor mass" is not uniquely defined. To avoid confusion, we use progenitor mass to refer to the initial mass of the BH progenitor unless we explicitly state otherwise (e.g. progenitor mass *at collapse*.)

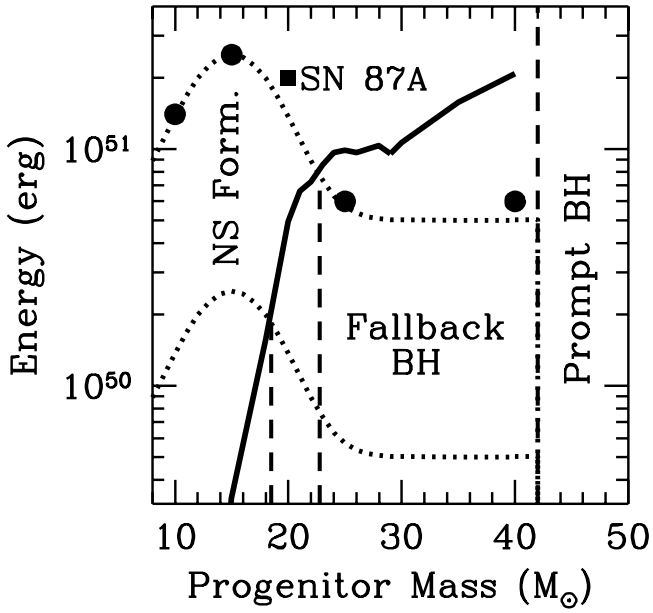

Fig. 1.— Explosion energy and binding energy as a function of hydrogen-rich progenitor mass. The circles are explosion energies calculated from core-collapse simulations (Fryer 1999a), while the square is the explosion energy inferred for SN 1987A (Woosley 1988). The upper dotted line is a fit to the numerical results for the explosion energy. Since only a fraction of the energy is used to unbind the star, we plot the lower dotted line, for which we assume that only 10% of the explosion energy actually goes into unbinding the star. The solid line is the binding energy of the entire stellar envelope outside the inner 3 $M_\odot$. The point at which the energy available to unbind the star crosses the binding energy marks the limit where BH formation occurs.

for 10% and 100% of the collapse energy being available to unbind the star, respectively. If the maximum NS mass is lower, as most equations of state in the literature predict (e.g., Cook, Shapiro, & Teukolsky 1994), the binding energies increase, and the critical progenitor masses decrease. The hydrogen envelope accounts for less than $\sim$ 10% of this total binding energy budget. Hence, if a star loses its hydrogen envelope before collapse but retains its helium core, its binding energy will not change by more than 10%.

Remnant mass. We can combine the estimated energies available to unbind the star and the stellar binding-energy profile (binding energy as a function of mass within the star) to calculate the remnant mass, $M_{\rm rem}$, as a function of progenitor mass, $M_{\rm prog}$:

$$f \times E_{\rm explosion} \;=\; \int_{M_{\rm rem}}^{M_{\rm prog}} E(m) dm, \qquad (2)$$

where f is the fraction of the total explosion energy used to unbind the outer layers of the star (down to $M_{\rm rem}$), and $E(m)$ is the binding energy profile. In this way, we can calculate the final remnant mass (and the amount of fallback) for a given progenitor mass. For $E(m)$ we use Woosley & Weaver (1995) massive star models. The remnant masses as a function of progenitor mass are shown in Figure 2 for $f = 0.1$ and $f = 1$. For very low explosion energies (high masses), most of the star falls back to form a black hole and

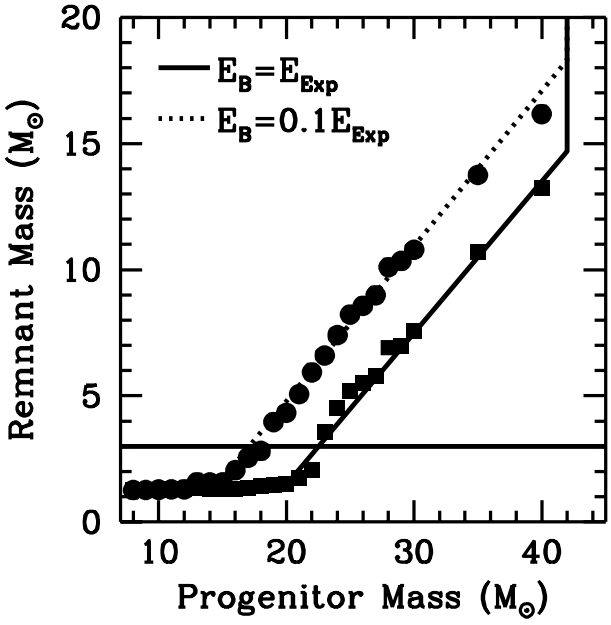

Fig. 2.— Compact remnant mass as a function of progenitor mass, assuming the energy, E_B, available to unbind the stellar envelope is equal to the explosion energy (solid line) or equal to 10% of the explosion energy (dotted line). For progenitors more massive than $40\,M_\odot$, there is no supernova explosion. The star collapses on itself and forms a black hole with mass equal to its progenitor mass.

the black hole mass is limited by the progenitor mass at collapse. In such cases, even if mass loss does not affect the explosion energy, it dictates the BH mass by limiting the total mass available to fall back and form a black hole (§2.2).

Initial mass function of progenitors. The final step in the calculation of a theoretical BH mass distribution requires the use of an initial mass function (IMF) for the massive BH progenitors, which we transform into a remnant mass function using the derived remnant-progenitor mass relation (Figure 2):

$$F(M_{\rm rem}) \;=\; F(M_{\rm prog}) \left(\frac{dM_{\rm rem}}{dM_{\rm prog}}\right)^{-1}. \qquad (3)$$

There is observational evidence that the IMF in the mass ranges of interest here is very well described by a single power law: $F(M_{\rm prog}) \propto M_{\rm prog}^{-\gamma}$ (for a Scalo IMF, $\gamma = 2.7$). Recent studies of massive stars claim a range of values for γ from 1.8 to 3.1 (see Massey & Thompson 1991) with no evidence for a dependence on metallicity (for massive stars). Because of this wide spread, we investigate a range of values for γ between 2 and 3 (Figure 3), while for most of the calculations we adopt $\gamma = 2.7$. The total number of BH is quite sensitive to γ (to the critical mass dividing NS and BH formation as well). Changing its value from 2 to 3 lowers the fraction of BH among core-collapse remnants from 30% to 12% (see Table 2, rows 1 and 2).

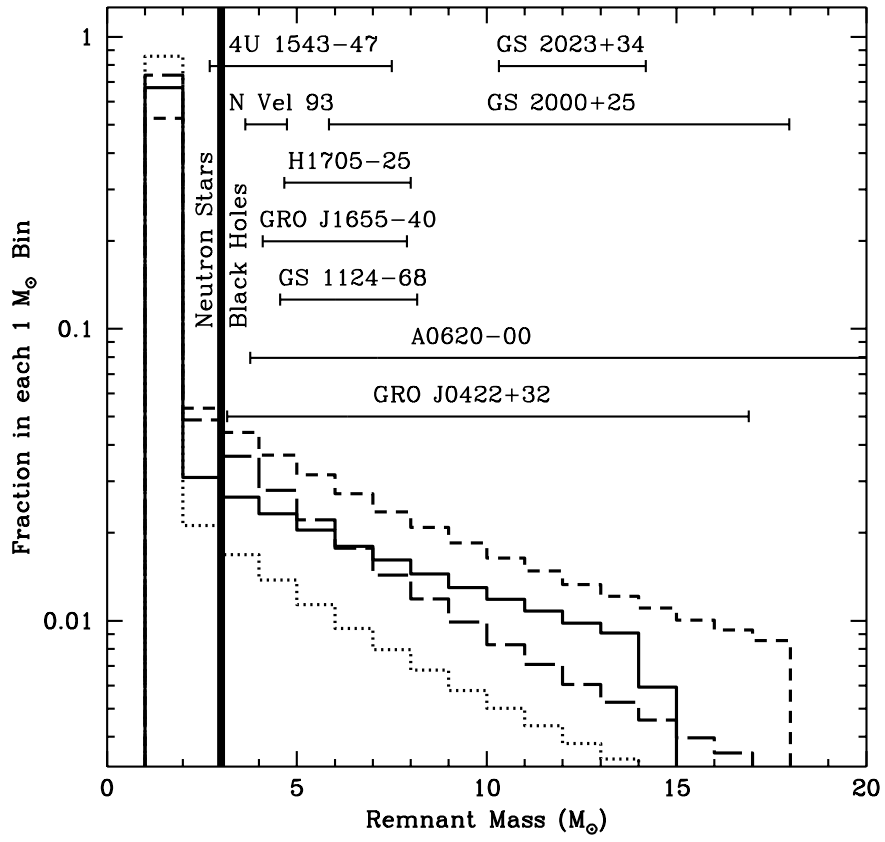

Fig. 3.— The mass distribution of compact remnants using the energies from Figure 1, for $f = 1$ (solid and dotted lines) and $f = 0.1$ (short- and long-dashed lines). We assume a power law initial mass function with indices $\gamma = 2.0$ (solid and short-dashed lines) and $\gamma = 3.0$ (dotted and long-dashed lines). Assuming the maximum NS mass is $\sim 3M_{\odot}$, we find that $\sim 80\%$ of compact remnants are neutron stars.

2.2. Results and Uncertainties

2.2.1. Supernova Energies and Remnant masses

The core-collapse simulations we use to derive explosion energies follow just the first ∼1s of the explosion (Fryer 1999a). In these models, the outward moving shock is still within the oxygen layer of the star at the end of the simulation. As the shock moves out of the star, a fraction of its energy is transformed into kinetic energy of the ejecta and another fraction goes into unbinding the core. Neutrino emission or absorption and nuclear burning and dissociation also contribute to the total energy budget but they represent only a minor fraction of it 1 s after bounce. In determining remnant masses we only need an estimate of the energy fraction, f, used to unbind the star. We vary this fraction between 0.1 and 1 and the total number of BH remnants changes by a factor smaller than 2 (Table 2, rows 1–4). Recent fallback models by MacFayden et al. (1999) suggest that f lies in the range 0.3–0.5. In most of our models we adopted $f = 0.5$.

The binding energy of stars at collapse is also difficult to determine. In the rotating stellar models by Heger, Langer & Woosley (1999), the binding energies (for matter outside the inner $3\,M_\odot$) are nearly a factor of two lower than those in the Woosley & Weaver (1995) non-rotating models The treatment of convection also introduces uncertainties in the binding energy. Currently, we are limited to the grid of pre-collapse stars produced by Woosley & Weaver (1995) and by the uncertainties in their assumptions for convection, rotation, etc. Lowering the binding energies of all stars by a factor of 2 is equivalent to raising f by a factor of 2. In this manner, varying f gives us an idea of the uncertainties caused by varying the magnitude of the binding energies. The trend of increasing binding energy with increasing mass is secure, and it is this trend that plays the most crucial role in our determination of the BH mass distribution determination.

The accuracy of the determined explosion energies depends on the current understanding of the supernova mechanism. Progress in this field indicates that the mechanism is sensitive to detailed physical processes and ingredients such as the equation of state, neutrino cross sections and transport, general relativity, and multi-dimensional effects (see Burrows 1998 and Mezzacappa 1999 for reviews). Until these are worked out, no "final" answer to the question of the explosion energy as a function of progenitor mass can be given. In fact, it is likely that for a given progenitor star mass, there is a range of possible supernova energies depending on the rotation of the progenitor (Fryer & Heger 1999). As with the binding energies, we can understand the effect of raising or lowering the explosion energy by varying f. More importantly, the trend of an increasing core-collapse energy up to a progenitor mass $\sim 15\,M_\odot$, followed by a decrease for more massive progenitors is expected to remain unchanged. To assess the effect of such uncertainties on the BH mass distribution, we vary the slope of this energy rise and decline (only the rate of decline is important for determining BH masses) with progenitor mass (Figure 4). We consider two cases, one of fast (dotted line) and one of slow (dashed line) decay compared to our standard case (Figure 1, top curve). The total number of black holes is not dramatically sensitive to the choice of this slope (Table 2, e.g., rows 5,11,12). However, the case of fast decline produces many more black holes with masses in excess of $10\,M_\odot$ (Table 2, Figs. 5, 6). For this simple case, the critical progenitor mass separating fallback and prompt BH formation decreases to $\sim 28\,M_\odot$ (Figure 5) from $\sim 40\,M_\odot$ for our standard case. We note that once we include the effects of stellar winds and close binary evolution (see § 2.2.2 and 2.2.3), the differences caused by varying the dependence of supernova energy on progenitor mass drops to the 20–30% level for the fraction of BH remnants in most mass ranges (Table 2). We ignore any mass loss that might occur after black hole formation (e.g. MacFayden et al.) because, at this time, we are unable to determine how often

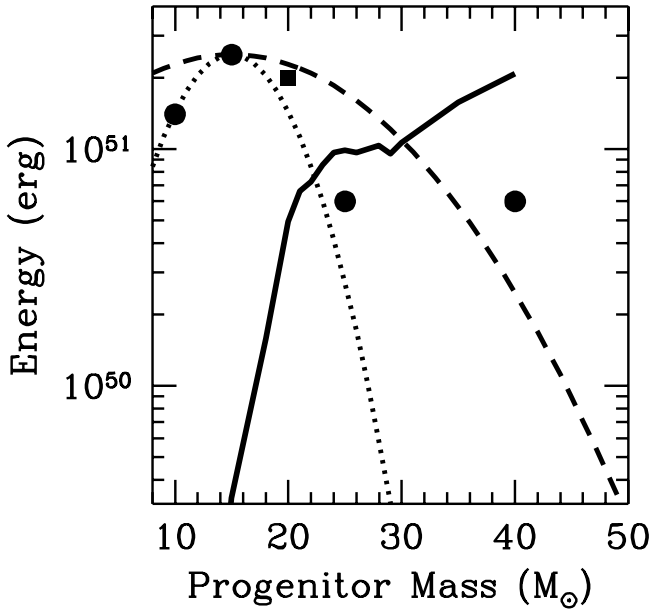

Fig. 4.— Explosion energy as a function of progenitor mass. The energy is assumed to rise and fall off faster (dotted line) and slower (dashed line) than our standard case (Figure 1, top curve). We plot the results from core-collapse simulations (circles) and SN 1987A (square) and the binding energy as a function of progenitor mass (solid line) for comparison.

(if at all) such explosions occur and do not know the amount of mass ejected even if an explosion occurs.

2.2.2. Wind Mass Loss from Single Stars

The physical processes driving winds for hydrogen stars and Wolf-Rayet stars are not entirely known and may be different for these two phases of mass loss. To study the effects of mass loss, we use the stellar models of Langer & Henkel (1995) and Schaller et al. (1992), who adopt different prescriptions for mass loss from hydrogen-rich and Wolf-Rayet stars.

Single stars less massive than $\sim 10\,M_\odot$ are not affected by winds. Stars with masses up to $\sim 40\,M_\odot$ lose a significant fraction of their hydrogen-rich envelope, most of it during the phase of core helium burning, but their cores remain largely unaffected by mass loss. Hence, the distribution of remnant masses from stars initially less massive than $\sim 40\,M_\odot$ are not sensitive to winds from single stars. More massive BH progenitors, however, experience such a dramatic decrease in their mass that they lose their entire hydrogen-rich envelope before they reach collapse. Further mass loss occurs during the strong Wolf-Rayet phase of the exposed helium cores. Wolf-Rayet winds considered in the models are strong enough to remove much of the helium core, causing most massive stars to form low-mass black holes (or even neutron stars). The remnant mass actually decreases as a function of initial progenitor mass (Figure 7, dotted line). However, since these massive progenitors are so rare, the primary effect of single-star winds on the BH mass

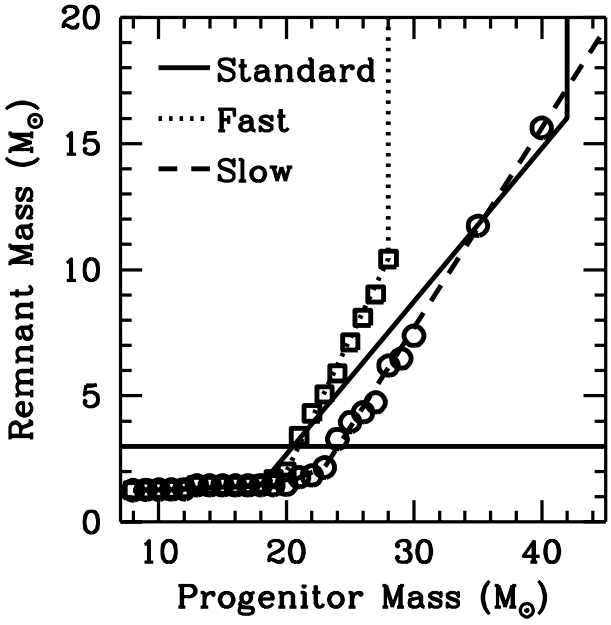

Fig. 5.— Remnant mass as a function of progenitor mass assuming that 50% of the explosion energy from Figures 1 and 4 is used to unbind the star. Three different cases for the slopes of rise and decline of the explosion energy are shown: standard (solid line), fast (dotted line) and slow (dashed line).

distribution is to limit the maximum BH mass to $\sim 12\,M_\odot$ (Figures 7 and 8) and to make the slope of the distribution roughly flat for remnant masses higher than $7\,M_\odot$ up to the maximum (Figure 8) . We note that for massive stars of lower metallicity, the wind loss rates are lower and therefore the maximum BH mass is higher.

2.2.3. Winds and Black Hole Progenitors in Binaries

So far, our discussion has been limited to single star evolution. However, BH masses are determined only in binaries. The short orbital periods of BH X-ray binaries (< 1 day to a few days, see Charles 1998) imply that their formation involves a common envelope phase (Kalogera 1999a). Therefore, to compare with the observations we must consider the effect of these *close* binaries on the BH mass distribution. A common envelope phase occurs when the BH progenitor star expands and transfers mass onto its companion. In many cases, the companion is engulfed by the BH progenitor and it spirals into the hydrogen envelope of the massive star, ejecting the hydrogen layers as it spirals inward. As a result, the mass of the BH progenitor at collapse decreases and consequently limits the BH remnant mass. Mass ejection because of binary evolution (e.g., common envelope) facilitates mass loss from winds by uncovering the helium core and causing even those BH progenitors with masses less than $40\,M_\odot$ to enter a high mass-loss, Wolf-Rayet phase. The importance of binary effects on the BH mass distribution depends upon how effective this Wolf-Rayet phase is at removing mass, which in turn, depends upon when the common envelope phase occurs (Woosley, Langer, & Weaver 1995). As we shall show in this section, this depends upon the separation of these

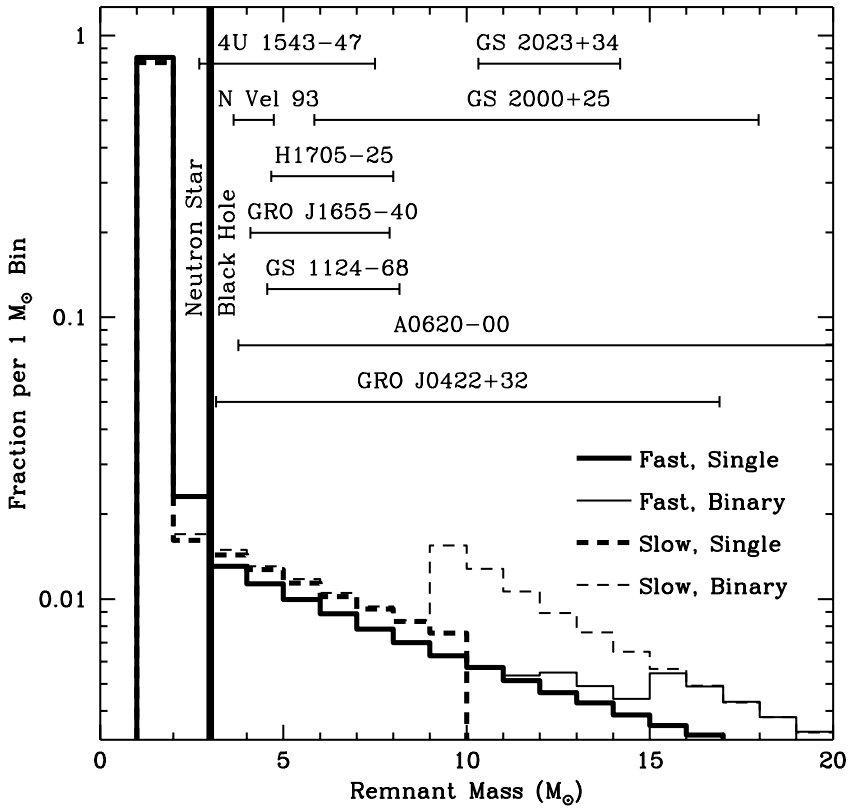

Fig. 6.— The mass distribution of compact remnants using the remnant–progenitor mass relation in Figure 5 and assuming an IMF with $\gamma = 2.7$. Line types are the same as in Figure 5.

binaries and our assumptions about the evolution of stellar radii.

In the *absence* of Wolf-Rayet winds, binary evolution merely limits the formation of very massive black holes (Figs. 7, 8). The hydrogen layers of the BH progenitor are ejected during common-envelope evolution, setting the mass of the star at collapse (and hence the maximum BH mass) equal to the mass of its helium core. If this occurs early in the progenitor's life, before the star goes through hydrogen shell burning, the helium-core masses tend to be somewhat smaller (by $\sim$1 $M_\odot$). However, this does not affect the inner core dramatically, and the explosion and binding energies of these binary BH progenitors are roughly the same as the values of single stars. The primary effect of binaries without winds is to constrain the black hole remnants of massive stars which undergo direct collapse (no explosion) to the mass of the helium core. This produces more black holes with masses between 10–20 $M_\odot$, but does not allow many black holes to be more massive than 20 $M_\odot$.

Our conclusion that in the absence of helium-star winds, the remnant masses do not depend on the presence or absence of a hydrogen envelope seems to contradict what has been stated in the past, for example by Woosley (1988), Herant & Woosley (1994), and Fryer (1999a). In these studies it was assumed that fallback was driven by the deceleration of the explosion shock as it enters the hydrogen envelope. The most recent simulations of fallback (MacFayden et al. 1999), indicate that the hydrogen envelope does not

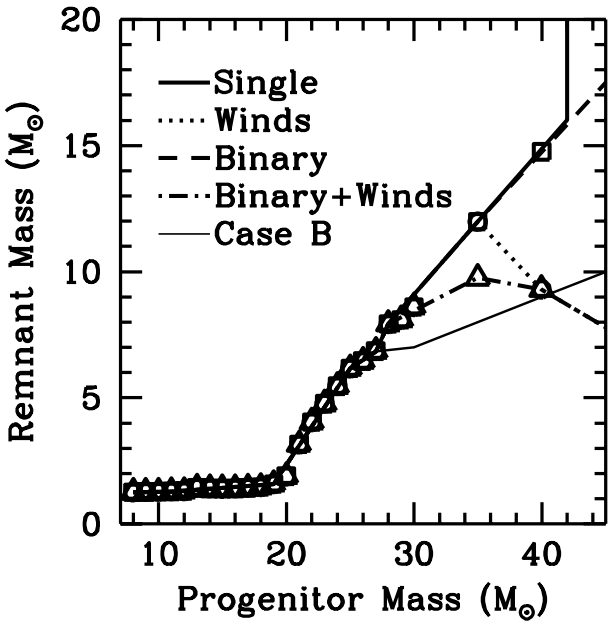

Fig. 7.— Remnant mass as a function of progenitor mass assuming 50% of the explosion energy from Figure 1 goes into unbinding the star. The different curves correspond to: single stars without winds (solid line), single stars with winds (dotted line), binaries without winds (dashed line), binaries with winds (dot-dashed line), and Case B (thin solid line).

influence the fallback process. Therefore we do not expect the hydrogen envelope to affect the amount of fallback except in the most massive stars, which in its presence would leave more massive remnants.

Because binaries facilitate the strong Wolf-Rayet winds by uncovering the helium cores of moderate-mass BH progenitors, winds are much more effective in binaries. As we discussed in §2.2.2, Wolf-Rayet winds significantly reduce remnant masses. For single stars, these winds only affect the very massive stars (and the very massive black hole remnants). However, in binaries, even stars less massive than $40\,M_\odot$ experience a Wolf-Rayet wind phase and this can affect the entire black hole mass distribution. The amount of mass lost depends upon when the BH progenitor loses its hydrogen envelope, that is, when mass transfer occurs. If it occurs before helium ignition (as the star expands off the main sequence), the star will lose mass during its entire helium burning phase. If mass transfer does not occur before helium ignition, it will not occur until after helium exhaustion because the star does not expand during helium burning (Schaller et al. 1992). After helium exhaustion, the star evolves so quickly that even the strong Wolf-Rayet winds currently assumed in the stellar models do not effect the mass significantly. We therefore have to consider separately BH progenitors that lose their hydrogen envelopes before (Case B mass transfer) or after (Case C mass transfer) core helium ignition.

With the current Wolf-Rayet mass-loss rates and models for helium star evolution, those BH progenitors which undergo Case B mass transfer will not form black holes. In this case, the exposed helium stars lose so much mass during the core helium burning that the BH progenitor's mass at collapse has decreased down to $\sim 3-4\,M_\odot$ (Woosley & Weaver 1995; Wellstein & Langer 1999). Such low-mass helium stars collapse to

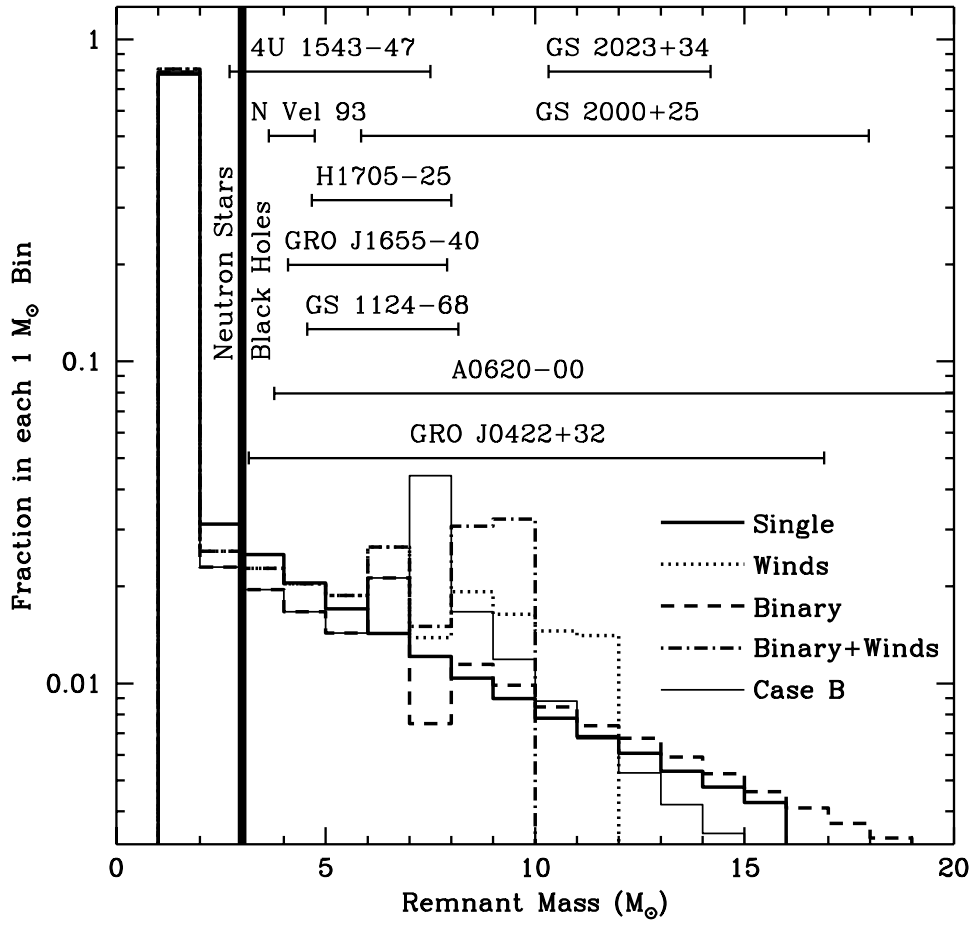

Fig. 8.— The mass distribution of compact remnants using the remnant–progenitor mass relation in Figure 7 and assuming an IMF with $\gamma = 2.7$. Line types are the same as in Figure 7.

NS and not BH, despite the fact that their initial progenitor mass exceeds $\sim 20\,M_\odot$.

If black holes cannot be formed in any massive binaries which undergo Case B mass transfer, the rate of BH formation decreases drastically (Portegies-Zwart, Verbunt, & Ergma 1997). To avoid Case B mass transfer, the orbit must be sufficiently wide to avoid mass transfer before helium ignition. But during core helium burning, winds cause the binary separation to widen even further, so the BH progenitor must expand significantly to undergo Case C mass transfer[2]. However, in typical stellar models of massive stars (e.g. Schaller et al. 1992), such expansion late in the evolution of the star occurs only for stars with initial masses below $\sim 25\,M_\odot$ (see also Kalogera & Webbink 1998). This produces a narrow range from 20 to $25\,M_\odot$ in which black holes could actually formed. Among binaries with primaries in the range $20 - 25\,M_\odot$, only a small fraction have orbits wide enough to avoid Case B mass transfer but also tight enough to go

[2]Recall that mass transfer must occur to tighten the binary orbit and produce the observed BH X-ray binaries.

through Case C evolution. This additional constraint is satisfied typically for orbital separations in the range $1600 - 1800\,R_\odot$ (Kalogera & Webbink 1998). The fraction of BH progenitors in binaries which satisfy all of these constraints is less than 1%! (Table 2, Row 8) In addition to this drastic reduction in the BH X-ray binary formation rate, the current stellar models face an even more serious problem: the black holes formed through this path are all less massive than $\sim 7\,M_\odot$ (helium core mass of a $25\,M_\odot$ star). Such an upper limit on the BH mass cannot account for systems like V404 Cyg (GS 2023+34) with its BH mass in the range $10 - 14\,M_\odot$.

Clearly something is wrong with the current stellar models. Either the current mass-loss rates from winds are too high or the radial evolution of stars is incorrect (Kalogera 1999b). We calculate BH mass distributions for two different possible cases: (i) the wind models for helium stars are correct but hydrogen rich stars more massive than $25\,M_\odot$ experience enough radial expansion after core helium exhaustion to evolve through Case C mass transfer, and (ii) the models for the late evolution of mass-losing massive stars are correct but wind mass loss for helium stars significantly weaker than assumed so far. Then helium stars exposed through Case B evolution lose smaller amounts of mass during core helium burning and at collapse are massive enough to form black holes.

If we assume that Wolf-Rayet wind models are correct, but that the radial evolution of stars are such that most stars undergo Case C mass transfer, we can explain the currently observed black hole binaries. In Case C mass transfer, the helium core is not uncovered until after helium exhaustion and the core collapses before any significant amount of mass is lost through a Wolf-Rayet wind (Wellstein & Langer 1999). Because these stars are in binaries, the maximum black hole mass is limited to the helium core mass. In addition, because we assume that the current models for winds are correct, stars more massive than $40\,M_\odot$ still lose much of their mass in winds, placing a further cap on the maximum black hole mass (Binary+Winds curve in Figs. 7, 8). With our choice in this case to ignore the current calculations for the radial evolution massive stars, we obtain a BH mass distribution where black holes make up ∼15% of all compact remnants (Table 2) and the maximum BH mass of $10\,M_\odot$ (just barely consistent with V404 Cyg).

Alternatively, it is possible that the true mass loss rates for helium stars are lower than what is estimated by Langer (1989) and used by Woosley, Langer, & Weaver (1995) amd Wellstein & Langer (1999). In fact, empirical estimates of Wolf-Rayet mass loss rates (Hamann & Koesterke 1998) have decreased with time. To investigate the effect of low Wolf-Rayet mass loss rates we calculate the BH mass distribution assuming that (i) 99% of the close binaries go through Case B evolution (and the remaining 1% go through Case C), and (ii) the amount of mass lost from the helium star by the time it reaches collapse is half of that calculated by Woosley, Langer, & Weaver (1995). This roughly corresponds to losing at most half of the initial helium-star mass (see Kalogera 1999a for constraints on the total amount of wind mass loss from helium stars). The corresponding mass distribution (Case B in Figs. 7, 8) produces black holes with masses in excess of $10\,M_\odot$ and can easily explain massive black holes such as V404 Cyg. However, this case may require a drastic reduction in the mass loss rate to cut the total mass lost by winds in half. Mass loss rates depend sensitively upon stellar luminosity and they decrease as the star loses mass. Decreasing the mass loss rate ($\dot{M}_{\rm wind}$) allows the star to retain its mass longer (and its high luminosity) and hence, it stays in a rapid mass-losing phase ($t_{\rm wind}$) longer. Since the total mass lost by winds is $\dot{M}_{\rm wind} \times t_{\rm wind}$, lowering the mass loss rate need not significantly lower the total mass lost (Wellstein & Langer 1999).

3. Discussion

In Table 2 we summarize our results for the range of theoretical BH mass distributions in terms of the percentage of BH among collapse remnants in different mass ranges. Despite the various uncertainties, some properties of the distributions are quite robust. In all examined cases we obtain a *continuous* remnant mass distribution that covers a wide range of values, from NS up to BH masses of at least 10–15 $M_\odot$. The form of the distribution is typically well described by an exponential of varying steepness, which in some cases is accompanied by an upper mass cut-off. We found no cases that lead to the formation of any kind of gaps in the distribution, although the appearance of valleys in the distribution in the range of $3-7\,M_\odot$ is possible (caused by winds and binaries - Fig. 8). The fraction of BH masses in the $3-5\,M_\odot$ range, varies from 15% to 30% and cannot be characterized as a gap. This fraction is mostly sensitive to the assumed power-law index γ of the massive-star IMF. The fraction of remnants in the $5-10\,M_\odot$ range is more sensitive to the assumptions about binaries and winds. It varies from 26-35%, 46-57%, 69-74% for single stars, single stars with winds, and binaries with winds, respectively. Finally the fraction of remnants in the $10-15\,M_\odot$ range is most sensitive to the assumptions about stellar winds. These assumptions also determine the existence and position of an upper BH mass cut-off.

Investigations of the observed sample of compact objects (Bailyn et al. 1998; Charles 1998) conclude that there is a discontinuous jump from NS to BH masses, that is, there exists a gap in the remnant mass distribution in the range $3-5\,M_\odot$. Bailyn et al. (1998) further found that the data (excluding V404 Cyg) appear to be consistent with a narrow BH mass distribution positioned at $\sim 7\,M_\odot$. Our results appear to be in disagreement with the conclusions in these studies. In what follows we address this disagreement in the light of a number of biases that may be operating and we derive some constraints on our theoretical limits.

There are three possible ways to resolve the apparent conflict between models and observations: i) the observed sample used by Bailyn et al. (1998) and Charles (1998) suffers from low-number statistics and larger samples will fill in the apparent gap at low BH masses and will best fit with broader distributions, (ii) there are biases operating against the identification or formation of X-ray binaries with low-mass BH, or (iii) one or more parts of the theoretical calculation presented here is incorrect.

Table 1 (and all the plots of our theoretical BH mass distributions) show the latest data on the mass estimates of the observed BH systems. Note that for 7 out of the 9 systems the measured BH mass ranges extend to values below $5\,M_\odot$. It is also important to point out that the current sample includes two very strong candidates for low-mass BH (Nova Velorum 1993 and 4U1543-47). These two systems have been observed only recently and were not included in the sample considered by Bailyn et al. (1998). In addition, new estimates of the mass of GRO J1655-40 predict a much lower limit for the black hole mass (Phillips, Shahbaz, & Podsiadlowski 1999). This result drastically changes the statistical analysis of Bailyn et al. (1998), which were dominated by the small error bars of GRO J1655-40 around a mass of $\sim 7\,M_\odot$. Taking all the above into account it is possible that the conclusions drawn from an earlier sample may not hold any longer.

Another possibility is that there is some observational selection effect against the identification of systems with low-mass black holes. The transient character is one example. Dynamical measurements of masses of the accreting objects in the systems studied so far can be made only during their quiescent phase so the source must be transient. Systems with lower-mass black holes will typically have mass ratios closer to unity (given the low mass companions, $< 1\,M_\odot$, observed) than the detected binaries. This will lead to higher mass transfer rates from the companions and it is reasonable to expect that these systems are actually persistent X-ray sources (and hence, mass measurements are hard to obtain). Such a trend has

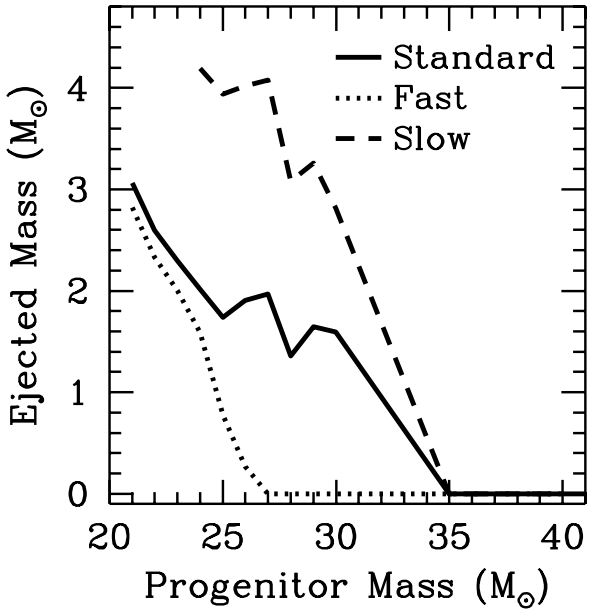

Fig. 9.— Mass ejected during BH formation as a function of progenitor mass for three different cases: our standard (SD) case from Figure 1 (solid line) and the cases of fast (dotted line) and slow (dashed line) rise/decline of the unbinding energy from Figure 4. We assume that 50% of the explosion energy is available to unbind the envelope and that both binary and wind effects (B+W) are taken into account.

been seen in the results obtained by King, Kolb, & Szuszkiewicz (1997) who studied the transient character of BH binaries. Systems with an unevolved low-mass companion ($\sim 1\,M_\odot$) move from unstable to the stable regime as the mass of the BH decreases below $5\,M_\odot$ down to $2\,M_\odot$.

In the context of biases against these systems, it is also possible that such systems have lower formation probability compared to higher-mass BH systems because of events in their formation that are not considered here, such as the effect of the BH formation (mass loss) on the binary characteristics. Using our results for the remnant mass as a function of progenitor mass (Figures 5, 7) we calculate the amount of mass lost during BH formation as a function of progenitor mass (Figure 9). It is evident that the formation of lower mass BH ($3 - 5\,M_\odot$) is associated with a higher fractional (relative to the progenitor or the BH) mass loss than the formation of $\sim 7\,M_\odot$ black holes. Although this mass loss is not enough to unbind the post-collapse system, even for the low-mass BH, it is enough to affect the size of the orbits after BH formation. We find that, the degree of orbital expansion immediately after the collapse in the case of $3\,M_\odot$ BH is higher than for $7\,M_\odot$ BH by a factor of $\simeq 3$. So binaries with low-mass BH tend to be wider than binaries with higher mass BH. Given the typical upper limit ($\sim 10\,R_\odot$) on orbital separation for systems to reach Roche lobe overflow (and hence enter an X-ray phase) (see Kalogera 1999a) and assuming a flat logarithmic distribution of separations, we estimate that the number of X-ray transients with $3\,M_\odot$ BH (and low-mass companions) is lower than that of $7\,M_\odot$ BH by $\sim 35\%$. We find that this fraction is sensitive to the form of the explosion energy dependence on progenitor mass (standard, slow or fast). However, this imbalance may not be high enough to account for a possible gap.

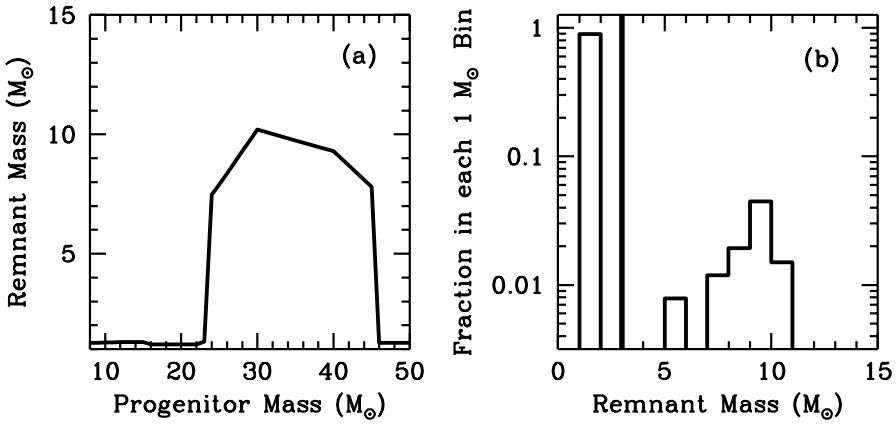

Fig. 10.— (a) Remnant mass as a function of progenitor mass and (b) distribution of remnant masses, assuming a step function for the dependence of explosion energy on progenitor mass. A gap in the range of 2–5 $M_\odot$ remnant masses appears (see text).

If the number of observed BH transients increases sufficiently to overcome the low-number statistics and observational biases, it is possible that it will support the existence of a gap in the range $3 - 5\,M_\odot$. Such a gap then could place strong constraints on the supernova explosion energy and its dependence on progenitor mass. One way a gap could be produced in the appropriate range of remnant masses is if the explosion energy behaves as a step function: e.g., $E_{\rm exp} = 2.5 \times 10^{51}$ ergs for $M_{\rm prog} < 23\,M_\odot$ and $E_{\rm exp} = 0$ ergs for $M_{\rm prog} > 23\,M_\odot$). For this distribution of supernova energies, a gap in the remnant masses in the range 2–5 $M_\odot$ appears (Figure 10). However, the observed range in supernova energies and our current understanding of the supernova mechanism both argue against supernova energies which follow a discrete step function in their dependence on progenitor mass, but a BH mass gap may force us to re-evaluate the current picture.

3.1. Neutron Star Mass Distribution

Although our focus in this paper is the BH mass distribution, it is still useful to examine our models with respect to what is known about NS masses. The NS mass distribution is more sensitive to core-collapse models and these results are somewhat more tentative than our BH mass distribution. As in the case of BH systems, a statistical examination of the measured NS masses shows that they are consistent with a very narrow distribution around 1.35 $M_\odot$ (Thorsett & Chakrabarty 1999). Note that the sample used in that study does not include recent results on Vela X-1 with a 2-sigma lower limit on its NS mass of $\sim$1.6 $M_\odot$ (Barziv et al. 1997; van Kerkwijk 1999, private communication). This narrow distribution agrees well with our predicted mass distribution (Figure 11). In our models, 81-96% of neutron stars lie in the mass range between 1.2–1.6 $M_\odot$. Beyond 1.6 $M_\odot$, there is a continuous distribution of neutron stars out to the maximum neutron star mass. The results are quite insensitive to the various uncertainties (explosion energy

behavior and fraction available to unbind the envelope, binary and wind effects). [3]. We would expect 1 or 2 neutron stars with masses beyond $1.6\,M_\odot$in the current data, and Vela X-1 seems to fall in this range. Our distribution is to be contrasted with that derived by Timmes, Woosley, & Weaver (1996), which has a double peaked neutron star distribution. Their distribution may also fit the observed sample of neutron stars with one peak explaining the cluster of neutron stars at $1.35\,M_\odot$, and the other fitting neutron stars such as Vela X-1. However, those results were obtained without considering the effects of fallback, which would smooth out the double-peaked distribution that was reported.

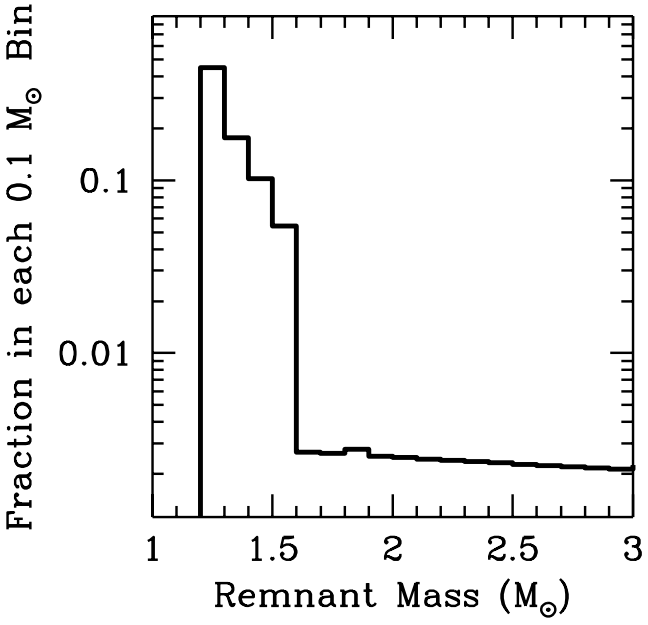

Fig. 11.— Distribution of neutron star remnant masses for our standard case for the explosion energy from Figure 1 ($f = 0.5$).

3.2. Effects of Winds and Binary Evolution

Our study demonstrates the strong sensitivity of the formation of massive black holes ($> 10\,M_\odot$) to the effects of winds. In close binaries (which form the observed black hole systems) these effects become even more extreme. In the simple case of single stars, winds alter the shape of the BH mass distribution by making it flatter and decreasing the maximum BH mass to $10-15\,M_\odot$. When the effect of a close companion is taken into account, winds drastically reduce the formation rate of BH and cause the maximum BH mass to decrease even further (at or below $10\,M_\odot$). Combined with the current stellar models (and in particular, the radial evolution of stars), theory can not explain the observed black hole systems (Kalogera 1999b). The

[3]However, the initial mass of the proto-neutron star (without fallback) is extremely sensitive to the supernova explosion mechanism which is not completely understood.

resolution of these problems lies either in significantly lowering mass loss rates, so that helium stars lose less than half of their initial mass (see also Kalogera 1999a), or in widening the range of both progenitor masses *and* binary orbital separations over which evolution through Case C mass transfer is allowed. The latter of the two possibilities would require that current estimates of stellar radii at the end of core helium burning in massive stars are actually *over*estimates *and* that the stellar radii just prior to collapse are actually *under*estimates, especially for stars more massive than $\sim 25\,M_\odot$. Given the uncertainties involved in theoretically determining the radii of evolved stars, such modifications are still possible. If revised stellar radii can not explain the black hole mass distribution, then the observed black hole masses require that mass loss from stellar winds must decrease. The downward trend of mass-loss rates from Wolf-Rayet winds (Hamann & Koesterke 1998) suggests that this may be the correct solution.

3.3. Neutron Star and Black Hole Kicks

The evidence that neutron stars receive kicks during their formation continues to grow (see Fryer, Woosley, & Hartmann 1999 for a review) and it is generally accepted that neutron stars must receive kicks with a mean velocity exceeding ∼100-200 $\mathrm{km\,s^{-1}}$ up to $\sim 400\,\mathrm{km\,s^{-1}}$. The question of BH kicks is still open however. Black hole X-ray binaries seem to have a Galactic distribution with a scale height smaller than that of NS X-ray binaries and an inferred mean velocity of only $\sim 40\,\mathrm{km\,s^{-1}}$ (White & van Paradijs 1996). Tutukov & Cherepaschuk (1997) and Nelemans et al. (1999) have argued that these velocities can be explained simply by mass ejection during BH formation and hence kicks are not necessary to explain the properties of BH binaries.

In constrast the majority of BH X-ray transients, GRO J1655-40 appears to have a large space velocity. Bailyn et al. (1995) measured its radial velocity to be $114\pm19\,\mathrm{km\,s^{-1}}$, which provides a lower limit to the space velocity. Under the assumption of isotropicity the measured radial velocity corresponds to a 3-D velocity of $\sim 200\,\mathrm{km\,s^{-1}}$. Phillips, Shahbaz, & Podsiadlowski (1999) were able to constrain the magnitude of the space velocity in the range $143 - 153\,\mathrm{km\,s^{-1}}$. Nelemans et al. (1999) used the current determinations of the BH mass and a relatively high mass for the BH companion and obtained space velocities of at most $110\,\mathrm{km\,s^{-1}}$ (just compatible with the radial velocity measurement). In their study the amount of mass loss was treated as a free parameter. However, as we discussed earlier in the paper, our calculations link the BH mass to the amount of mass lost during BH formation. We use our results for the full set of cases (different dependence of explosion energy on the progenitor mass and different values of the parameter f) and find that space velocities in the range $100 - 200\,\mathrm{km\,s^{-1}}$ require pre-collapse orbital separations ($0.1 - 4\,R_\odot$) too small to accommodate the BH companion in the binary. Imposing this latter constraint, we obtain maximum space velocities, for the different models, in the range $20 - 85\,\mathrm{km\,s^{-1}}$. We conclude that the measured radial velocity of GRO J1655-40 seems to require that a kick was imparted to the BH (in agreement also with Brandt et al. 1995). Given that the majority of the systems appear to have low space velocities (White & van Paradijs 1996), Fryer (1999b) found that a BH kick of at least $\sim 50\,\mathrm{km\,s^{-1}}$ is required to explain the velocities of the complete set of BH X-ray transients.

We have shown here that most of the black holes are formed via fallback and not promptly. Since many of the NS kick mechanisms operate before fallback occurs, it seems reasonable to expect that BH receive kicks as well. Given the kick mechanisms, it is likely that the momentum imparted by asymmetric explosions is equal for both BH and NS, and therefore the kick scales with mass: $< V_{\rm BH} >=< V_{\rm NS} > M_{\rm NS}/M_{\rm BH}$. If this is the case, then lower mass BH will receive higher kicks. This, in the context of a possible gap in the low-mass BH range, possibly provides an additional bias against the formation of low-mass BH in binaries.

We find that, for a typical NS kick magnitude of $200\,\mathrm{km\,s^{-1}}$ and for reasonable values of post-CE orbital separations, 25%–50% (for a fixed BH kick magnitude of $50\,\mathrm{km\,s^{-1}}$ the fraction is in the range 10%-50%) of the systems with $3\,M_\odot$ BH get disrupted while systems with $7\,M_\odot$ BH remain unaffected. This effect could contribute to decreasing the formation frequency of X-ray binaries with low-mass black holes.

We thank N. Langer, S. Wellstein, and A. Heger for useful discussions. The work of CLF was supported by NASA (NAG5-8128) and the US DOE ASCI Program (W-7405-ENG-48). VK acknowledges support by the Smithsonian Institution in the form of a CfA Postdoctoral Fellowship.

REFERENCES

Bailyn, C.D., et al. 1995, Nature, 378, 157

Bailyn, C. D., Jain, R. K., Coppi, P., & Orosz, J. A. 1998, ApJ, 499, 367

Barziv, O., Kaper, L., van Paradijs, J., & van Kerkwijk, M.H. 1997, at the Joint European and National Astronomical Meeting, JENAM-97, held in Thessaloniki, Greece, 2-5 July, 1997

Beekman, G., Shahbaz, T., Naylor, T., Charles, P.A., Wagner, R.M., & Martini, P. 1997, MNRAS, 290, 303

Brandt, W.N., Podsiadlowski, P., & Sigurdsson, S. 1995, MNRAS, 277, L35

Burrows, A. 1998 to be published in the proceedings of the 9'th Workshop on Nuclear Astrophysics, held at the Ringberg Castle, Germany, March 23-29, ed. E. Müller & W. Hillebrandt

Charles, P.A. 1998, in Theory of Black Hole Accretion Disks, eds. M.A. Abramowicz, G. Bjornsson & J.E. Pringle, (Cambridge: Cambridge University Press), 1

Colgate, S.A. 1971, ApJ, 163, 221

Cook, G.B., Shapiro, S.L., & Teukolsky, S.A., 1994, ApJ, 424, 823

Filippenko, A.V., Leonard, D.C., Matheson, T., Li, W., Moran, E.C., Riess, A.G 1999, PASP, 111, 969

Fryer, C.L. 1999a, ApJ, 522, 413

Fryer, C.L. 1999b, to appear in the proceedings of the IAU symposium "Highly Energetic Physical Processes and Mechanisms for Emissions from Astrophysical Plasmas", eds. P.C.H. Martens and S. Tsuruta

Fryer, C.L., & Heger, A. 1999, submitted to ApJ[astro-ph/9907433]

Fryer, C.L., Woosley, S.E., & Hartmann, D. 1999, ApJ, in press [astro-ph/9904122]

Hamann, W.-R., & Koesterke, L. 1998, A&A, 335, 1003

Harlaftis, E., Collier, S., Horne, K., & Filippenko, A.V. 1999, A&A, 341, 491

Heger, A., Langer, N., & Woosley, S. E. 1999, ApJ, in press

Herant, M., & Woosley, S.E. 1994, ApJ, 425, 814

Kalogera, V., & Baym, G. 1996, ApJ, 470, L61

Kalogera, V., & Webbink, R.F. 1998, ApJ, 493, 351

Kalogera, V. 1999a, ApJ, 521, 723

Kalogera, V. 1999b, to appear in Black Holes in Binaries and Galactic Nuclei, ESO Workshop, eds. L. Kaper, E. P. J. van den Heuvel

King, A.R., Kolb, U., & Szuszkiewicz, E. 1997, ApJ, 488, 89

Langer, N. 1989, A&A, 220, 135

Langer, N., & Henkel, C. 1995, Space Science Reviews, 74, 343

MacFayden, A., Woosley, S.E., & Heger, A. 1999, submitted to ApJ

Massey, P., & Thompson, A.B. 1991, AJ, 101, 1408

Mezzacappa, A. 1999, to appear in the Memoirs of the Italian Astronomical Society as the Proceedings of Future Directions of Supernova Research: progenitors to remnants, September 29-October 2, 1998, Gran Sasso

Nelemans, G., Tauris, T.M., & van den Heuvel, E.P.J. 1999, A&A, in press

Orosz, J.A., Jain, R.K., Bailyn, C.D., McClintock, J.E., & Remillard, R.A. 1998, ApJ, 499, 3750

Phillips, S.N., Shahbaz, T., & Podsiadlowski, Ph. 1999, MNRAS, 304, 839

Portegies-Zwart, S.F., Verbunt, F., & Ergma, E. 1997, A&A, 321, 207

Rhoades, C.E.Jr., & Ruffini, R. 1974, Phys. Rev. Lett., 32, 324

Schaller, G., Schaerer, D., Meynet, G., & Maeder, A. 1992, A&A, 96, 269

Shahbaz, T., van der Hooft, F., Casares, J., Charles, P.A., & van Paradijs, J. 1999, MNRAS, 306, 89

Thorsett, S.E., & Chakrabarty, D. 1999, ApJ, 512, 288

Timmes, F.X., Woosley, S.E., & Weaver, T.A. 1996, ApJ, 457, 834

Tutukov, A.V., & Cherepaschuk, A.M. 1997, Astronomicheskij Zhurnal, 74, 407

Wellstein, S., & Langer, N. 1999, submitted to A&A[astro-ph/9904256]

White, N.E., van Paradijs, J. 1996, ApJ, 473, L25

Woosley, S.E. 1988, ApJ, 330, 218

Woosley, S.E., Langer, N., & Weaver, T.A. 1995, ApJ, 448, 315

Woosley, S.E., & Weaver, T.A. 1995, ApJS, 101, 181

Table 1. Measured Black Hole Masses[a]

System	Mass Range ($M_\odot$)
GS 2023+34 (Nova Cyg 1938/1989) (V404 Cyg)	10.3-14.2[b]
GS 2000+25 (Nova Vul 1988)	5.84-18.0
H1705-25 (Nova Oph 1977)	4.67-8.00
GRO J1655-40 (Nova Sco 1994)	4.1-7.9[c]
GS 1124-68 (Nova Mus 1991)	4.56-8.17
A0620-00 (Nova Mon 1975) (V616 Mon)	3.78-25.4
GRO J0422+32 (Nova Per 1992)	3.16-16.9[d]
GRS 1009-45 (Nova Vel 1993) (V1234 Oph)	$\sim$3.64-4.74[e]
4U1543-47	$\sim$2.7-7.5[f]

[a]We do not include the high mass X-ray binaries (Cyg X-1, LMC X-1, LMC X-3), whose masses are much less certain than those obtained in X-ray transients.

[b]Unless otherwise stated, data are taken from Bailyn et al. (1998).

[c]The lower limit for the black hole mass comes from the analysis of Phillips, Shahbaz, & Podsiadlowski (1999). The upper limit comes from the revised mass function of Shahbaz et al. (1999).

[d]We have included the revised mass ratio and mass function from Harlaftis et al. (1999). Note that Beekman et al. (1997) have argued that the BH mass in this system may be much larger than our upper limit ($\gtrsim 28 M_\odot$). They argue that the inclination angle is much lower than past estimates.

[e]This system is not yet studied in detail (Filippenko et al. 1999) and the error bars may be revised in the future.

[f]Like Nova Vel 1993, this system is not yet studied in detail (Orosz et al. 1998).

Table 2. Black Hole Masses

Model Parameters			Percentage of BH Compact Remnants $\equiv N_{\rm BH}/(N_{\rm BH}+N_{\rm NS})$				
Energy[a]	Winds[b]	IMF[c]	Total	3-5$M_\odot$	5-10$M_\odot$	10-15$M_\odot$	>15$M_\odot$
SD, 100%	—	2.0	29.9	5.0	8.2	4.7	12
SD, 100%	—	3.0	12.1	3.1	4.1	1.9	3.0
SD, 10%	—	2.0	42.1	8.1	12.2	6.8	15.0
SD, 10%	—	3.0	21.3	6.5	7.6	3.1	4.1
SD, 50%	—	2.7	19.1	4.6	6.3	3.1	5.1
SD, 50%	B	2.7	18.5	3.6	6.4	3.4	5.1
SD, 50%	W	2.7	16.7	4.3	9.5	2.9	0
SD, 50%	B+W*	2.7	0.088	0.043	0.045	0	0
SD, 50%	B+W	2.7	16.6	4.3	12.3	0	0
SD, 50%	Case B	2.7	18.5	3.6	10.4	2.9	1.5
Slow, 50%	—	2.7	14.2	2.4	4.0	2.4	5.4
Fast, 50%	—	2.7	18.4	2.7	4.7	0.30	10.7
Slow, 50%	B	2.7	14.2	2.4	4.0	2.6	5.2
Fast, 50%	B	2.7	18.2	2.8	5.6	4.6	5.2
Slow, 50%	W	2.7	12.4	3.1	7.1	2.2	0.
Fast, 50%	W	2.7	16.5	3.4	7.6	2.7	2.8
Slow, 50%	B+W	2.7	12.3	3.2	9.1	0.	0.
Fast, 50%	B+W	2.7	16.4	3.6	11.3	1.5	0.

[a]Explosion Energy: SD≡standard rise/fall slope – see Figure 1, Slow, Fast≡slow, fast rise/fall slope – see Figure 4. 10,50,100%: Fraction of explosion energy available to eject material – see Figure 1.

[b]Winds, Binary Effects: —≡no winds or binary effects, B≡binary effects only, W≡Wind effects only, B+W* ≡ Winds+Binaries (stellar radii from literature), B+W≡Winds + Binaries (all binaries in Case C), Case B≡Winds + Binaries (almost all binaries in Case B); see text.

[c]Initial Mass Function power law γ, see text.